Real-Time Direct Measurement Method of Power System Frequency

Hongzhi Chen and He Chen, *Student Member, IEEE*

***Abstract*—Accurate measurement of grid frequency timely is essential to the stable operation of a grid network and the performance of a grid-connected converter. When harmonic pollution exists in the power system, indexes of timeliness, accuracy, and noise rejection performance are required to be considered synthetically. However, these indexes are usually difficult to be taken care of at the same time, and problems of convergence and stability should also be considered. In order to calculate grid frequency precisely and timely, this paper proposes a grid frequency measurement method. A three-level function of the grid voltage signal is defined step by step. On the basis of the function, equations with the signal's frequency and amplitude as two unknowns are established. Finally, a system of equations is obtained and solved in order to calculate grid frequency. The proposed method calculates grid frequency precisely through strict theoretical derivation, possesses a strong anti-disturbance ability against harmonics, and is simple for realization. In addition, because of the absence of iteration and feedback calculation, problems of convergence property as well as stability do not exist. Effectiveness of this method is proved through simulation and experiment.**

***Index Terms*—Frequency measurement, frequency estimation, signal processing, power systems.**

I. Introduction

BECAUSE power systems often operate close to their stability limits, frequency deviation is likely occur due to multiple reasons including load shedding, generation-load mismatches, etc. Inaccurate frequency information can jeopardize the efficiency as well as safety of grid networks [1]–[3]. Moreover, frequency is one of the most important information required by grid-connected converters in the process of synchronization. If frequency is poorly estimated, harm might not only be caused to the converters, harmonic wave pollutions can also be brought to grid networks. Consequently, accurate measurement of frequency with distorted and noisy signals in power systems is a challenging problem that has attracted numerous attention [4]–[8].

Manuscript received March 13, 2018; revised October 14, 2018 and March 27, 2019; accepted June 9, 2019. Date of publication June 19, 2019; date of current version October 24, 2019. Paper no. TPWRS-00362-2018. *(Corresponding author: Hongzhi Chen.)*

H. Chen is with the College of Information Science and Engineering, Northeastern University, Shenyang 110819, China (e-mail: chenhongzhi@mail.neu.edu.cn).

H. Chen is with the Laboratory for Computational Sensing and Robotics, Johns Hopkins University, Baltimore, MD 21210 USA (e-mail: hchen136@jhu.edu).

Color versions of one or more of the figures in this paper are available online at http://ieeexplore.ieee.org.

Digital Object Identifier 10.1109/TPWRS.2019.2923784

Currently, frequency measurement methods can be summarized into two categories, namely direct calculation methods and estimation methods.

Methods such as zero-crossing point detection and three equidistant samples calculate the frequency precisely. In these direct calculation methods, frequency is measured with simple calculation processes, has a fast dynamic response, and the problem of stability need not to be worried about. However, these methods tend to be easily affected by harmonics and noises in signals to be measured. In order to improve the accuracy of frequency measurement with noises, improvements are proposed in literatures [8], [9]. But complexity of calculation is increased to some degree.

Frequency estimation methods can be subdivided into two types: iteration methods and close-loop regulation methods. Methods including Discrete Fourier Transform (DFT), Fast Fourier Transform (FFT) are typical iteration methods [10]–[15]. In the process of estimating frequency with Fourier Transformation, iteration link is required to be designed. Similar iteration methods include D-Estimation Method [16], Recursive Least Squares (RLS) [17], and adaptive method [18]. These methods mainly stress the accuracy and dynamic response speed of frequency estimation. A well-designed iteration scheme can obtain high accuracy at the same time taking the dynamic response speed into consideration. However, these methods are usually not real time, and their application is mainly in the monitoring of power system. Close-loop regulation methods, such as those adopting Phase Lock Loop (PLL) [19], [20], aim at realizing grid-synchronization, and measurement of parameters including frequency is realized by close-loop control. These methods are usually applied in the real time control of grid-connected converters, and real time feature and dynamic performance are usually stressed under the condition that basic accuracy requirement is met.

The two frequency estimation methods have different application fields, but they also have common features as following. Firstly, both methods have noise rejection ability to some degree. Secondly, both methods estimate the frequency of the signal and make the estimated value approaches the actual value gradually. However, convergence condition could not be avoided for iterative computation, and the topic of stability has to be confronted for feedback regulation. In order to take multiple indexes including measurement accuracy, convergence, and stability into consideration, complexity and difficulty for frequency measurement would be increased.

In order to overcome aforementioned difficulties confronted by frequency measurement algorithms, this paper proposes a direct frequency calculation method. Aiming at overcoming the problems of convergence and stability, iteration and close-loop regulation are absent in this method. Aiming at enhancing the noise rejection capability, shift time window is adopted to obtain the data of test signal. Calculation model of frequency is constructed, and binary equations with two unknowns of the frequency and amplitude of test signal are derived. On the basis of these equations, systems of equations can be extracted, and frequency can be obtained by solving the systems of equations.

II. Principle of Frequency Measurement

In order to obtain the frequency of the measured periodical signal, the following work is carried out. Firstly, one-level functions with the variable of the measured signal are defined; Afterwards, seeing the one-level functions as variables, at the same time introducing an adjustable parameter, we define two-level functions; Then, considering the two-level functions as variables, at the same time introducing another adjustable parameter, three-level function is constructed. On the basis of the defined function set, equations with measured signal's frequency and amplitude as two unknowns can be determined by regulating the two adjustable parameters. Finally, a system of equations is established, and the frequency of fundamental wave in the measured signal is obtained.

A. Definition of the Function Set

Suppose the measured signal as $x(t) = U\sin(2\pi f_1 t + \theta)$ with its instantaneous values known, while its frequency f_1, amplitude U, as well as initial phase θ are unknown.

We introduce reference sine and cosine signals, namely $\sin(2\pi f_1{}^* t)$ and $\cos(2\pi f_1{}^* t)$. The period of the reference signals is $T = 1/f_1{}^*$. Define one-level function with the variable of the measured signal.

$$\begin{cases} X_a(t) = k\int_{t-T}^{t} x(\tau)\cos(2\pi f_1^*\tau)d\tau \\ X_b(t) = k\int_{t-T}^{t} x(\tau)\sin(2\pi f_1^*\tau)d\tau \end{cases} \tag{1}$$

where k can take the value of any real number except for zero.

Specifically, in order to avoid confusion of adjustable parameters and variables, we represent functions in the form of $f(\mathrm{x}; y)$, where x before the semicolon represents adjustable parameter and y after the semicolon represents variable. All the functions in this paper are defined following this principle.

Considering the one-level functions $X_a(t)$ and $X_b(t)$ as variables and introducing an adjustable parameter α, a two-level function is defined.

$$\begin{cases} P(\alpha;t) = X_a(t)X_a(t-\alpha T) + X_b(t)X_b(t-\alpha T) \\ Q(\alpha;t) = X_a(t)X_b(t-\alpha T) - X_b(t)X_a(t-\alpha T) \end{cases} \tag{2}$$

where $X_a(t-\alpha T)$ and $X_b(t-\alpha T)$ respectively represents the lag function of $X_a(t)$ and $X_b(t)$ with the lag time of $\alpha\, T$.

Considering the two-level functions $P(\alpha;\ \mathrm{t})$ and $Q(\alpha;\ t)$ as variables and introducing an adjustable parameter φ, a three-level function is defined as

$$F_{pq}(\varphi,\alpha;t) = \cos\varphi P(\alpha;t) + \sin\varphi Q(\alpha;t) \tag{3}$$

So far, we have finished defining three-level function. In the following, the method of solving problems with the defined function set is discussed. Because $F_{pq}(\varphi,\alpha;t)$ is the function of functions, we can consider it in another perspective for the convenience of analysis: $P(\alpha;\ t)$, $Q(\alpha;\ t)$, $X_a(t)$, and $X_b(t)$ are considered as intermediate variables, all of which contain $\mathrm{x}(t)$. f_1, U, and θ are parameters of $x(t)$ whose values are unknown, thus they can also be considered as arguments of $F_{pq}(\varphi,\alpha;t)$. Consequently, $F_{pq}(\varphi,\alpha;t)$can be written in another way:

$$F_{pq}(\varphi,\alpha;t) = F(\varphi,\alpha;t,f_1,U,\theta) \tag{4}$$

Because $F(\varphi,\ \alpha;\ t, f_1,\ \mathrm{U},\ \theta)$ contains the argument t, it's difficult to obtain the value of f_1 directly. Thus, in order to calculate f_1, our aim should be getting an equation that is related to f_1 and U but unrelated to t.

Aiming at realizing the above goal, two adjustable parameters φ and α are set. In the following, we try to find a condition under which $F(\varphi,\ \alpha;\ t, f_1,\ U,\ \theta)$ is unrelated to t and θ. We assume that condition is $\varphi = \varphi_0$ and $\alpha = \alpha_0$. Under this circumstance, an equation is expected to be constructed as

$$F(\varphi_0,\alpha_0;f_1,U) = F_{pq}(\varphi_0,\alpha_0;t) \tag{5}$$

whose left side only contains the variables f_1 and U, while absent of the variables t and θ, and the right side is a value that can be calculated real time through equations (1)–(3). If an equation like that presented in (5) can be constructed, real time frequency measurement problem can be simplified into the problem of solving the system of equations.

B. Establishment of Equations With Frequency and Amplitude as Two Unknowns

Based on the aforementioned three-level function set, now we begin seeking for the equations with frequency and amplitude as two unknowns. First of all, one-level function is expanded and simplified, and the simplification result is substituted into the two-level function. Next, similar process is carried out on the two-level function, namely expanded and simplified, and the simplification result is substituted into the three-level function. Finally, similar process is carried out on the three-level function, and equations with frequency and amplitude as two unknowns are established through observation and analysis of the simplification result.

By expanding and simplifying equation (1), the following equation is obtained

$$\begin{cases} X_a(t) = A\sin(2\pi(f_1+f_1^*)t+\theta-\pi f_1 T) \\ \qquad\quad +B\sin(2\pi(f_1-f_1^*)t+\theta-\pi f_1 T) \\ X_b(t) = -A\cos(2\pi(f_1+f_1^*)t+\theta-\pi f_1 T) \\ \qquad\quad +B\cos(2\pi(f_1-f_1^*)t+\theta-\pi f_1 T) \\ A = kU\sin(\pi f_1 T)/(2\pi(f_1+f_1^*)) \\ B = kU\sin(\pi f_1 T)/(2\pi(f_1-f_1^*)) \end{cases} \tag{6}$$

In equation (6), A and B are introduced for the convenience of expression. Substituting equation (6) into equation (2),

after simplification, the equations shown in (7) at the bottom of this page can be obtained.

Substitute equation (7) into equation (3), after simplification, it can be gained that

$$\begin{aligned} F_{pq}(\varphi,\alpha;t) = {} & A^2\cos(2\pi\alpha f_1 T + 2\pi\alpha + \varphi) + B^2 \\ & \cos(2\pi\alpha f_1 T - 2\pi\alpha - \varphi) - 2AB\cos(4\pi f_1 t \\ & + 2\theta - 2\pi f_1 T - 2\pi f_1 \alpha T)\cos(2\pi\alpha + \varphi) \end{aligned} \quad (8)$$

Observing equation (8), the right side contains three contributions, and the third contribution contains time variable *t*. When $2\pi\alpha + \varphi = n\pi + \pi/2$ (n = 0,1,2,3,…), $\cos(2\pi\alpha + \varphi)$ equals zero, so the third contribution equals zero. In this way, equation (8) has the first two contributions left. After further simplification, it can be gained that

$$\begin{cases} 2\pi\alpha + \varphi = n\pi + \pi/2 \ \ (n = 0, 1, 2, \cdots,) \\ F_{pq}(\varphi,\alpha;t) = (-1)^n (B^2 - A^2)\sin(2\pi\alpha f_1 T) \end{cases} \quad (9)$$

From equation (9), the right side of the equation contains variable f_1. Combining equation (6), it's not difficult to find that *A* and *B* contains variables f_1 and *U*. The left side of equation (9) represents values of $F_{pq}(\varphi,\alpha;t)$ calculated in real time. Consequently, equation (9) equals the equations with frequency and amplitude as two unknowns that we are seeking for.

In order to adapt to the habit expression that unknowns are placed on the left side of equations, we exchange the left side with the right side of equation (9). To avoid confusion, expressions of *A* and *B* are also presented here, and equation (9) can be changed to the form bellow

$$\begin{cases} 2\pi\alpha + \varphi = n\pi + \pi/2 (n = 0, 1, 2, \cdots,) \\ (-1)^n (B^2 - A^2)\sin(2\pi\alpha f_1 T) = F_{pq}(\varphi,\alpha,t) \\ A = kU\sin(\pi f_1 T)/(2\pi(f_1 + f_1^*)) \\ B = kU\sin(\pi f_1 T)/(2\pi(f_1 - f_1^*)) \end{cases} \quad (10)$$

In equation (10), when one pair of adjustable parameters (φ, α) satisfying the condition $2\pi\alpha + \varphi = n\pi + \pi/2$ is selected randomly, one equation with two unknowns of f_1 and *U* can be obtained correspondingly. Since there exist infinite pairs of (φ, α), the corresponding equations are also infinite. Consequently, equation (10) can be seen as a set of equations with two unknowns of f_1 and *U*. If we select two equations from this set at (φ, α) and (φ_2, α_2) and build a system of two equations, it's not difficult to solve the values of f_1 and *U*. When choosing (φ, α) to establish the equations, we should make sure it's convenient to calculate the solutions, which are based on inverse trigonometric function like $\sin^{-1}()$, $\cos^{-1}()$ and $\tan^{-1}()$.

C. Derivation of Frequency Measurement Method

Because multiple methods of frequency and amplitude measurement exist based on equations (10) and (1)–(3), there's no need to enumerate them here. We choose one example to present the process.

Two or more equations can be selected to construct the system of equations for frequency solving. This example selects three equations to do that from the perspective of noise rejection ability. The three parameter pairs of (φ, α) selected are respectively (0, 1/4), (π/2, *n*/2), and (π/2, *n*/2–1/2). The corresponding system of equations is constructed as

$$\begin{cases} (B^2 - A^2)\sin((1/2)\pi f_1 T) = F_{pq}(0, 1/4; t) \\ (-1)^n (B^2 - A^2)\sin(n\pi f_1 T) = F_{pq}(\pi/2, n/2; t) \\ (-1)^{n-1}(B^2 - A^2)\sin((n-1)\pi f_1 T) \\ \quad = F_{pq}(\pi/2, (n-1)/2; t) \end{cases} \quad (11)$$

In order to solve the system of equations, we carry out the calculation of (① + ③) ÷ (2 × ①) for equation (11)

$$\begin{aligned} & \frac{(-1)^n(\sin(n\pi f_1 T) - \sin((n-1)\pi f_1 T))}{2\sin((1/2)\pi f_1 T)} \\ & = \frac{F_{pq}(\pi/2, n/2; t) + F_{pq}(\pi/2, n/2 - 1/2; t)}{2F_{pq}(0, 1/4; t)} \end{aligned} \quad (12)$$

From equation (12), the frequency calculation equation can be derived as

$$\begin{cases} f_1 = f_1^* + 2f_1^*/((2n-1)\pi)\sin^{-1}\phi \\ \phi = \frac{F_{pq}(\pi/2, n/2; t) + F_{pq}(\pi/2, (n-1)/2; t)}{2F_{pq}(0, 1/4; t)} \end{cases} \quad (13)$$

After frequency is calculated, it's not difficult to derive the solving equation of amplitude from equation (10), (11). Because this paper focuses on the problem of frequency measurement, no further discussion of amplitude measurement is presented here.

D. Realization of the Frequency Measurement Method

Realization process of the frequency measurement method is shown by the following 5 steps:

1) Set the values of adjustable parameter α, and reference frequency $f_1{}^*$, and parameter *k*.
2) Data of *x*(*t*) during (*t* − *T*, *t*) is stored, based on which the data of $X_a(t)$ and $X_b(t)$ can be calculated according to equation (1). And the values of $X_a(t)$ and $X_b(t)$ during $(t - \alpha_{max}T, t)$ is stored. α max represents the maximum value of α used in the calculation process, and it is set as *n*/2 in this example.
3) According to the data of $X_a(t)$ and $X_b(t)$ saved in the former step and equation (2), the values of *P*(1/4; t), *Q*(*n*/2; *t*), *Q*(*n*/2−1/2; *t*) are calculated.

$$\begin{cases} P(\alpha;t) = A^2\cos(2\pi f_1\alpha T + 2\pi\alpha) + B^2\cos(2\pi f_1\alpha T - 2\pi\alpha) \\ \qquad -2AB\cos(4\pi f_1 t + 2\theta - 2\pi f_1 T - 2\pi f_1\alpha T)\cos(2\pi\alpha) \\ Q(\alpha;t) = -A^2\sin(2\pi f_1\alpha T + 2\pi\alpha) + B^2\sin(2\pi f_1\alpha T - 2\pi\alpha) \\ \qquad +2AB\cos(4\pi f_1 t + 2\theta - 2\pi f_1 T - 2\pi f_1\alpha T)\sin(2\pi\alpha) \end{cases} \quad (7)$$

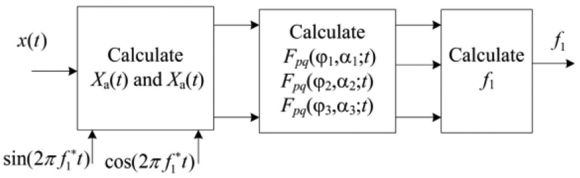

Fig. 1. Diagram from frequency operation.

4) According to equation (3), the values of $F_{pq}(0, 1/4; t)$, $F_{pq}(\pi/2, n/2; t)$, $F_{pq}(\pi/2, n/2 - 1/2; t)$ are calculated.
5) According to equation (13), the value of frequency is calculated.

Based on the procedures above, the block diagram of frequency measurement is drawn, as shown in Fig. 1.

In order to evaluate the frequency measurement performance thoroughly, analysis of noise rejection ability of the proposed method needs to be carried out.

III. Analysis of Noise Rejection Ability

In the proposed frequency measurement method, no special filter link is required. The harmonic inhibition ability is actually hidden in the calculation of intermediate variables. $F_{pq}(\varphi, \alpha; t)$ is the variable directly used for frequency calculation, thus the harmonic inhibition ability is effectively realized in the values of $F_{pq}(\varphi, \alpha; t)$. In the following, analysis is carried out from the perspective of $F_{pq}(\varphi, \alpha; t)$ calculation.

Firstly, equation (1) is performed. This process can be seen as superposition of modulation and integral. By modulation, we are referring to the multiplication of reference sinusoidal signals with $x(t)$. By integral, amplitude of the signal with similar frequency of ${f_1}^*$ is strengthened, while the other frequency components are weakened. In other words, the function of a filter is realized.

Secondly, equation (2) is performed. Signals from the result of equation (1) are further filtered, which means stronger signals are further strengthened while weaker signals are further weakened.

Thirdly, equation (3) is performed, whose calculation result aims at calculating the value of $F_{pq}(\varphi, \alpha; t)$ and transforming the result of equation (2) into dc component.

In summary, the proposed method has strong noise rejection ability.

IV. Analysis of Parameter Selection Principle

Parameters that require selection include k, ${f_1}^*$, α, φ, and n. It's important to discuss the effect of parameter design on the frequency measurement method. It's not difficult to see from the calculation result of $F_{pq}(\varphi, \alpha; t)$ from equation (9) that only three of these parameters affect the calculation of $F_{pq}(\varphi, \alpha; t)$, namely k, ${f_1}^*$, and α. While parameters φ and n serve to assist the adjustment of α in the process of solving f_1. Analysis of the impact of parameters k, ${f_1}^*$, and α on frequency measurement can be realized by analyzing their effect on $F_{pq}(\varphi, \alpha; t)$. In the proposed direct calculation method, two of the most important performance indexes are respectively precision and dynamic response speed. It can be observed from the relationship between $F_{pq}(\varphi, \alpha; t)$ and test signal $x(t)$ that the larger the amplitude of $F_{pq}(\varphi, \alpha; t)$ is, the higher precision of measurement is, under the circumstance that $x(t)$ has a fixed amplitude. In the following, analysis of the impact of parameters on $|F_{pq}(\varphi, \alpha; t)|$ is carried out to determine the relationship between parameter selection and frequency measurement precision.

When the value of k increases, the precision of measurement is increased, while the signal-to-noise ratio would not be increased. But the computation burden would also be increased with the increase of k. Consequently, the value of k should be selected as a moderately large one. This paper selects $k = 2/T$. The values of ${f_1}^*$ and α determine the impact of frequency value on $|F_{pq}(\varphi, \alpha; t)|$. Deeper analysis is required to observe such impact. According to equation (9), the calculation expression of $|F_{pq}(\varphi, \alpha; t)|$ can be represented as bellow

$$\begin{cases} |F_{pq}(\varphi, \alpha; t)| = (B^2 - A^2)\,|\sin(2\pi\alpha f_1 T)| \\ B^2 - A^2 = \left(\frac{kUT}{2}\frac{\sin(\pi f_1 T)}{\pi(f_1 - f_1^*)T}\right)^2 \\ \qquad\quad - \left(\frac{kUT}{2}\frac{\sin(\pi f_1 T)}{\pi(f_1 + f_1^*)T}\right)^2 \end{cases} \tag{14}$$

It can be seen from equation (14) that $|F_{pq}(\varphi, \alpha; t)|$ is related to U, f_1, k, α, ${f_1}^*$. When the value of k is fixed, Δf ($\Delta f = f_1 - {f_1}^*$) is the offset value of frequency. Such relationship can be described as the relationship between $|F_{pq}(\varphi, \alpha; t)|$ and U, f, α. In order to show such relationship clearly, per-unit form of f is presented, and the magnification of $F_{pq}(\varphi, \alpha; t)$ is defined as $M(\alpha,\delta)$. We have,

$$\begin{cases} k = 2/T \\ f_1 = (1 + \delta){f_1}^* \\ |F_{pq}(\varphi, \alpha; t)| = M(\alpha, \delta)U^2 \end{cases} \tag{15}$$

where $M(\alpha, \delta)$ represents the magnification of amplitude, δ represents per-unit value of f. Substitute equation (15) into equation (14), we have

$$M(\alpha, \delta) = \left(\left(\frac{\sin(\delta\pi)}{\delta\pi}\right)^2 - \left(\frac{\sin(\delta\pi)}{2\pi + \delta\pi}\right)^2\right)|\sin(2\pi(1 + \delta)\alpha)| \tag{16}$$

In fact, the selection of δ equals the selection of ${f_1}^*$. In the following, analysis is carried out for the relationship between parameter selection and precision. It should be noted that measurement error does not exist in the proposed method theoretically, but digital realization might bring error unavoidably. Precision of frequency measurement can be enhanced by increasing the value of $F_{pq}(\varphi, \alpha; t)$, which can be realized by increasing the value of $M(\alpha, \delta)$.

In order to observe the relationship among $M(\alpha, \delta)$, δ and α, simulation is carried out. Fig. 2 shows the figure plotted from equation (16). The pattern of Fig. 2 shows the range of δ and α within which $M(\alpha, \delta)$ has relatively larger value.

It can be seen from Fig. 2 that relatively larger $M(\alpha, \delta)$ corresponds to δ within the range of $[-1, 1]$, namely the test signal

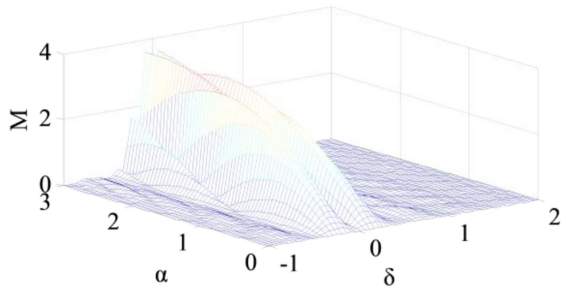

Fig. 2. M(α, δ).

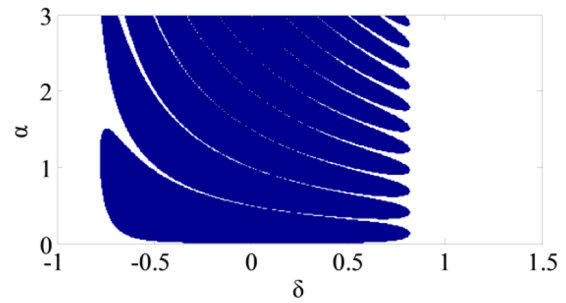

Fig. 3. The area of M(α, δ) $\geq$ 0.04.

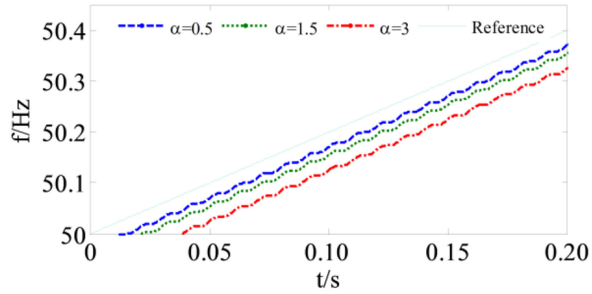

Fig. 4. Responses of proposed method for df/ dt = 2 Hz/s.

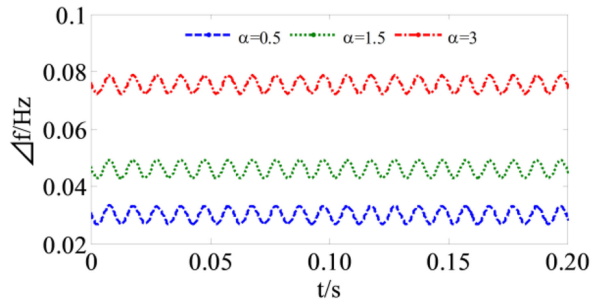

Fig. 5. Frequency tracking error.

$x(t)$ should be in the range of 0 to 2 $f_1{}^*$. In order to observe the ranges of parameters more clearly, planar slice diagram of Fig. 2 with the condition that $M(\alpha, \delta) \geq 0.04$ is given in Fig. 3.

Shadowed area in Fig. 3 represents $M(\alpha, \delta) \geq 0.04$. To ensure the precision of frequency measurement, α and δ should be chosen inside the shadowed area. It could also be noted from the figure that component of test signal $x(t)$ that locates outside the range of 0 to $2f_1{}^*$ can be seen as noise signal, and its influence on precision is little.

Except for precision, dynamic response speed of frequency measurement should also be taken into consideration. As calculation delay composes the main part of response time, dynamic response speed can be estimated from the delay of calculating process from test signal $x(t)$ to $F_{pq}(\varphi, \alpha; t)$. The process can be divided into two parts: Firstly, $X_a(t)$ and $X_b(t)$ are calculated from $x(t)$ with a delay of $T/2$; Secondly, $P(\alpha; t)$ and $Q(\alpha; t)$ are calculated from $X_a(t)$ and $X_b(t)$ with a delay of $\alpha T/2$. Consequently, delay of the whole process is appropriately $(1 + \alpha)T/2$. To calculate grid frequency, multiple values of $F_{pq}(\varphi, \alpha; t)$ would be required, as shown in equation (13). It should be noted that among these values if $F_{pq}(\varphi, \alpha_{max}; t)$ has the maximum value of α, its delay would also be maximum. In other words, define the actual delay as T_d, $T_d \approx (1 + \alpha_{max})T/2$.

V. Simulation Research

Simulation is carried out to verify correctness and effectiveness of the above theoretical analysis. Specifically, dynamic response speed and noise rejection ability of the proposed method is verified. The relationship between the value of α and frequency measurement performance is determined. Under the circumstance that harmonic noises is absent, the impact of parameter variation on dynamic response speed and steady state precision is studied. Under the circumstance that harmonic noises exist, the impact of parameter variation on noise rejection ability is studied. Set parameters as $f_1{}^* = 50$ Hz. $k = 100$. Comparative simulation is presented with α_{max} taking three different values, namely 0.5, 1.5, and 3.

A. Frequency Ramp Test

Set the test signal as:

$$\begin{cases} x(t) = 100\sin(2\pi f t) \\ f = 2t, 49 \leq f \leq 51 \end{cases}$$

This simulation is used to test the delay of the frequency measurement method when the parameters take different values. Moreover, the difference between actual value and estimated value of the delay is compared.

Simulation result is shown in Figs. 4 and 5. Fig. 4 shows the reference frequency and the measured frequency when the parameter takes three different values. Fig. 5 shows the waveforms of frequency measurement errors when the parameter takes three different values.

It can be seen from Fig. 4 that delay exists in the proposed frequency measurement method, and delay increases with the increase of α_{max}.

Calculation of delay is designed as bellow: Variation rate of the test signal is df/dt = 2. If the measurement error of frequency is Δf, the actual value of delay can be calculated by

$$T_d = \Delta f \,(df/dt) \tag{17}$$

While the estimated delay can be calculated by

$$T_{de} = (1 + a_{\max})\, T/2 \tag{18}$$

TABLE I
RELATION BETWEEN PARAMETER α AND DELAY TIME

α_{max}	T_d	T_{de}
0.5	15 ms	15 ms
1.5	23 ms,	25 ms
3.0	37.5 ms	40 ms

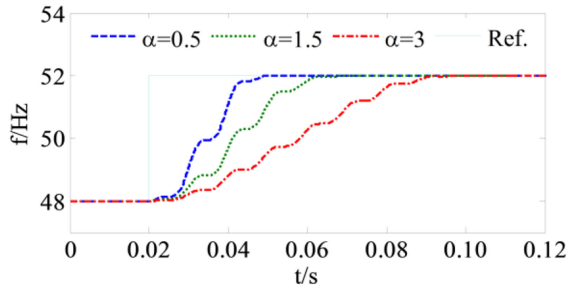

Fig. 6. Dynamic responses of proposed method for +4 Hz frequency step.

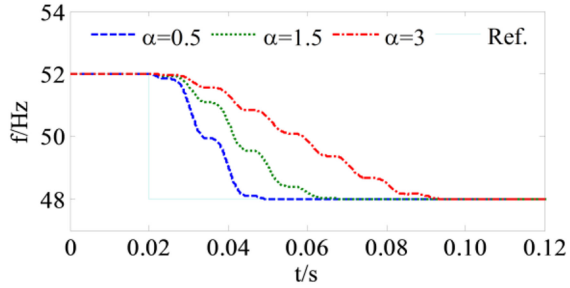

Fig. 7. Dynamic responses of proposed method for −4 Hz frequency step.

Calculating the values of T_d and T_{de} from the above analysis, Table I can be obtained.

It can be seen from Table I that the values of T_d are close to those of T_{de}. Consequently, in the design of frequency measurement method, in order to determine the T_d that meets the demand of dynamic response speed, T_{de} can be used to replace T_d and then parameters can be chosen accordingly.

B. Frequency Step Test

Set the test signal as

$$\begin{cases} x(t) = 100\sin(2\pi f t) \\ f = 48 + 4\cdot 1(t-1) - 4\cdot 1(t-2) \end{cases}$$

Fig. 6 shows the waveforms of measured frequency when the signal of test signal steps up. Fig. 7 shows the waveforms of measured frequency when the signal of test signal steps down. It can be seen from the figures that dynamic response speed decreases with the increase of α_{max}. In the dynamic changing process, overshoot does not exist. Transient process time equals $(1+\alpha_{max})T$.

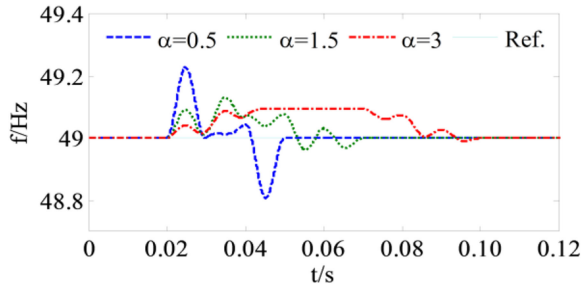

Fig. 8. Dynamic responses of proposed method for +10% magnitude step.

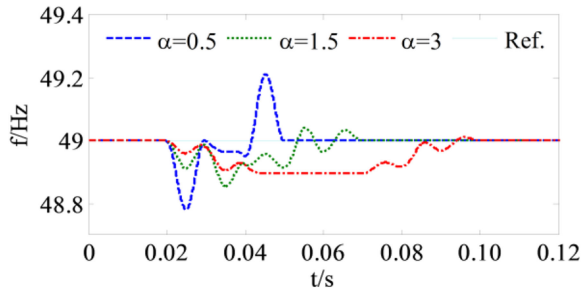

Fig. 9. Dynamic responses of proposed method for −10% magnitude step.

C. Magnitude Step Test

Set the test signal as

$$\begin{cases} x(t) = U(t)\sin(98\pi t) \\ U(t) = 100 + 10\cdot 1(t-1) - 10\cdot 1(t-2) \end{cases}.$$

Fig. 8 shows the dynamic responses of the proposed method for +10% magnitude step, while Fig. 9 shows that for −10% magnitude step. It can be seen from Figs. 8 and 9 that when α_{max} increases, the magnitude of frequency decreases, and the adjustment time is lengthened.

D. Noise Rejection Test

Because derivation of the proposed method is obtained when noise is absent, noise rejection ability of the proposed method requires further verification. In the following, simulations are carried out in two different aspects.

1) Simulation Result With the Existence of DC Noise Rejection: Set the test signal as

$$x(t) = 100\sin(102\pi t) + 10.$$

Fig. 10 shows the simulation result. It's not difficult to observe from Fig. 10 that dc noise does not affect the precision of frequency measurement when the parameter takes different values.

2) Simulation Result With the Existence of Various Harmonic Noise: Set the test signal as

$$x(t) = 100\sin(102\pi t) + 10 + 5\sin(2\times 102\pi t) + 10\sin(3\times 102\pi t).$$

Fig. 11(a)–(c) respectively shows the simulation results with parameter α_{max} taking the value 0.5, 1.5, and 3. It can be

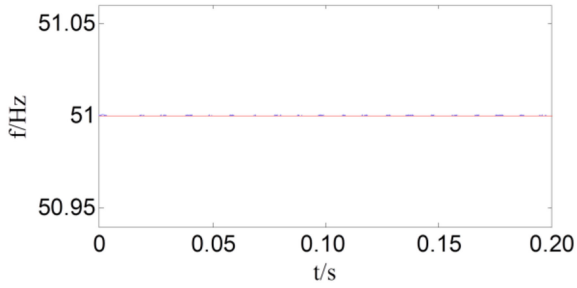

Fig. 10. Measured frequency with DC noise.

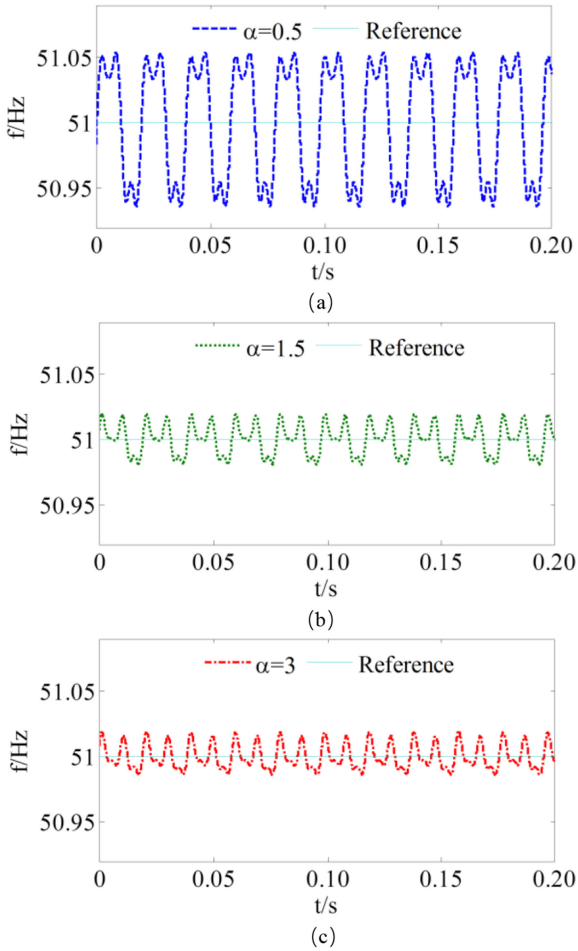

Fig. 11. Measured frequency with harmonic noise.

observed from Fig. 11 that frequency can be measured precisely under the three circumstances. The amplitude of ripple decreases with the increase of α_{max}, which suggests that harmonic noise rejection ability enhances with the increase of α_{max}.

E. Frequency Modulation Test

Set the test signal as

$$\begin{cases} f(t) = 50 + 2\sin(4\pi t) \\ \vartheta = 2\pi \int_0^t f(\tau)d\tau \\ x(t) = 100\sin\vartheta \end{cases}$$

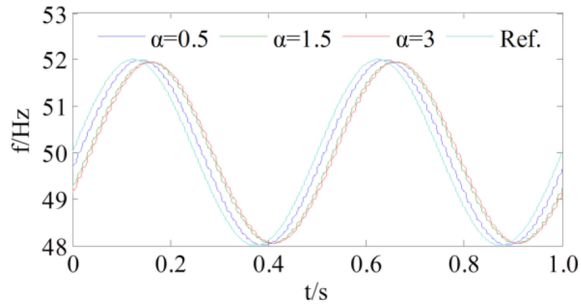

Fig. 12. Measured frequency of proposed method for modulation.

TABLE II
COMPARISON OF FREQUENCY MEASUREMENT RESULTS

frequency	frequency-estimation RMS error	
	RFEM algorithm(n=2)	Proposed algorithm (αmax=1. 5)
46 Hz	613 mHz	500 mHz
47 Hz	348 mHz	248 mHz
48 Hz	94 mHz	95 mHz
49 Hz	47 mHz	41 mHz
50 Hz	92 mHz	0 mHz
51 Hz	104 mHz	45 mHz
52 Hz	72 mHz	100 mHz
53 Hz	200 mHz	211 mHz
54 Hz	265 mHz	322 mHz
55 Hz	269 mHz	522 mHz
56 Hz	351 mHz	620 mHz
estimation time	24.7 ms	20 ms

Because the frequency of the signal to be measured varies with time, we represent the frequency as $f(t) = 50 + 2\sin(4\pi t)$. In this expression of frequency, the basis is 50. The overlapped signal upon the basis is a sinusoidal signal which has an amplitude of 2 and a frequency of 2 Hz. So the frequency is centered at 50, with a variation between 48 and 52 in the form of sinusoidal pattern. Set $\alpha = 0.5$, $\alpha = 1.5$, $\alpha = 3$ respectively, and the simulation result is shown in Fig. 12.

In Fig. 12, the four curves are respectively reference frequency and measured result when $\alpha = 0.5$, $\alpha = 1.5$, and $\alpha = 3$. It can be seen from the simulation result that the proposed algorithm can measure the frequency precisely, with a delay from the reference signal. And the larger α is, the larger delay is.

F. Comparison With Published Methods

In addition, to further evaluate the algorithm in this paper, we carry out a comparison between the proposed method, and methods in [9] and [11].

The authors of [9] proposed Robust Frequency-Estimation Method (RFEM). Firstly, the square of test signal is calculated, and 10 filters connected in serial are used, 8 of which are order-adjustable filters. Secondly, frequency is calculated according to the filtering result. Setting the order of filter as 2, comparison experiment is carried out for RFEM and the proposed method with the same test signal. Table II shows RMS of the frequency

TABLE III
COMPARISON OF FREQUENCY MEASUREMENT RESULTS

frequency	frequency-estimation error	
	TDFT algorithm	Proposed algorithm (αmax=0. 5)
40 Hz	113 mHz	600 mHz
42 Hz	97 mHz	550 mHz
44 Hz	-13 mHz	400 mHz
46 Hz	-81 mHz	210 mHz
48 Hz	-65 mHz	54 mHz
50 Hz	0 mHz	0 mHz
52 Hz	49 mHz	48 mHz
54 Hz	47 mHz	165 mHz
56 Hz	6 mHz	265 mHz
58 Hz	-50 mHz	310 mHz
60 Hz	-97 mHz	308 mHz
estimation time	20 ms	15 ms

measurement error as well as time consumed for frequency estimation. In the test signal of Table II, the components of different harmonics are distributed as: 5% third harmonic, 6% fifth harmonic, 5% seventh harmonic, 1.5% ninth harmonic, 3.5% eleventh harmonic, 2% thirteenth harmonic, 0.5% fifteenth harmonic, and 2% seventeenth harmonic.The sampling frequency of this test was set to 5 kHz. It can be observed form Table II that the proposed method outperforms RFEM in both frequency measurement precision and speed, especially in the range between 48 Hz∼52 Hz. Moreover, the proposed method has simpler structure, thus more applicable in realistic situation.

In [11], transformed discrete Fourier transform (TDFT) is used for frequency estimation. Comparison experiment is carried out between the proposed method and TDFT with the same test signal. Table III shows the peak value of frequency measurement error and the time consumed fore frequency estimation. In the test signal used in Table III, components of different harmonics are distributed as: 5% third harmonic, 2% fifth harmonic, and 1% seventh harmonic. The sampling frequency of this test was set to 3.2 kHz. It can be seen from Table III that in the range of 48 Hz∼52 Hz, the method proposed in this manuscript has similar performance with TDFT. Out of that range, the proposed method has slightly larger measurement error than TDFT. However, it should also be noted that the proposed method consumes less time than TDFT.

VI. EXPERIMENT RESULTS

In order to verify effectiveness of the proposed method, the following hardware prototype is constructed. A 16-digit A/D is used to sample tested signal with a frequency of 5 kHz. For implementing the frequency measurement algorithm, DSP chip TMS320F28335 manufactured by Texas Instrument is adopted. The output of the DSP chip is then input into a 14-digit D/A. Test signal required in the experiments is generated by a D/A chip.

Experimental results are given in Figs. 13–17. Figs. 13 and 14 are experimental results when the frequency of test signal experiences a step change. Figs. 15 and 16 are experimental

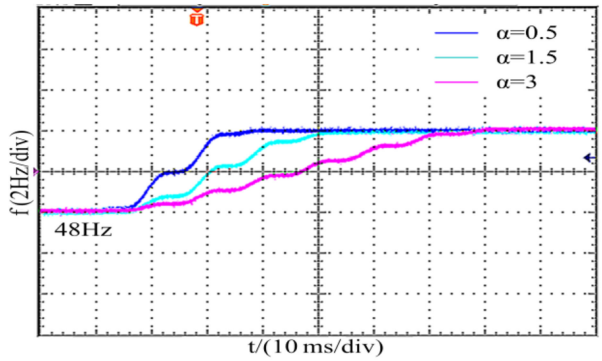

Fig. 13. Dynamic responses of proposed method for +4 Hz frequency step.

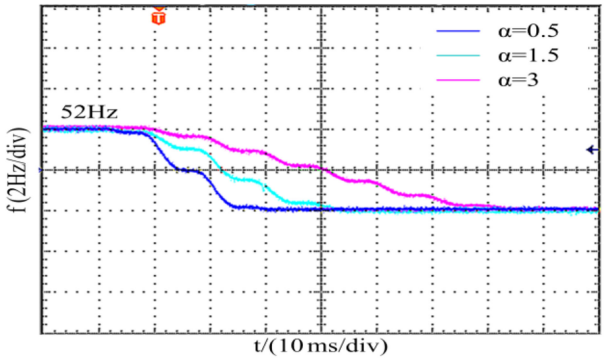

Fig. 14. Dynamic responses of proposed method for −4 Hz frequency step.

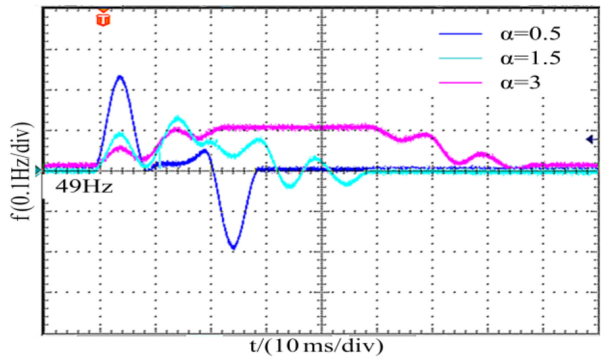

Fig. 15. Dynamic responses of proposed method for+10% magnitude step.

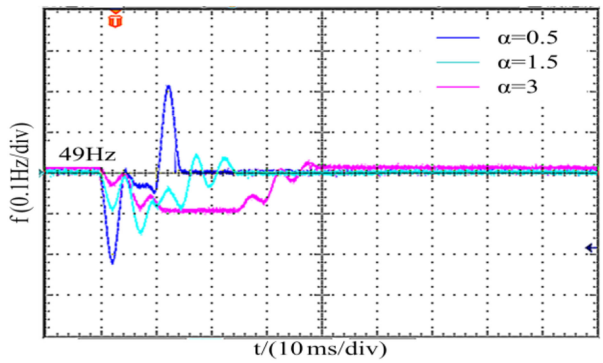

Fig. 16. Dynamic responses of proposed method for −10% magnitude step.

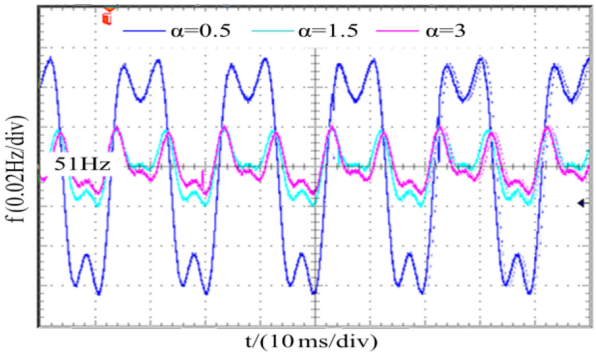

Fig. 17. Measured frequency with harmonic noise.

results when the amplitude of test signal. Fig. 17 shows the experimental results of steady state when disturbance is existent.

Experimental results show that, the proposed method is effective in real time frequency measurement, and is feasible in application.

VII. Conclusion

This paper constructed a basic mathematical tool for frequency and amplitude measurement of periodical functions with equations (1)–(3) and (10). Various specific methods can be generated based on this mathematical tool, and optimization of these methods is a prospective topic remains to be discussed.

The proposed method can eliminate the impact of dc noise, and has a strong capability of harmonic noise rejection. Moreover, the relationship between parameter selection and dynamic response speed is analyzed, and the problem of stability does not exist. Another feature of the method is that since it is a real time method, application is not restricted to monitoring of power system, but can be applied in the field of the control of grid-connected converters. It should be noted that as a mathematical tool, the proposed frequency measurement method is not restricted to the field of grid frequency measurement, it can also be applied to measure the frequency and amplitude of other periodical functions by adjusting the frequency of reference sine and cosine signals.

References

[1] D. Fan and V. Centeno, "Phasor-based synchronized frequency measurement in power systems," *IEEE Trans. Power Syst.*, vol. 22, no. 4, pp. 2010–2016, Oct. 2007.

[2] D. H. Dini and D. P. Mandic, "Widely linear modeling for frequency estimation in unbalanced three-phase power systems," *IEEE Trans. Instrum. Meas.*, vol. 63, no. 2, pp. 353–363, Feb. 2013.

[3] R. Malpani, Z. Abbas, and K. S. Swarup, "High precision frequency estimation using internet-based phasor measurement unit," *IEEE Trans. Power Syst.*, vol. 25, no. 2, pp. 607–614, May 2010.

[4] P. Rodriguez, A. Luna, R. S. Muñoz-Aguilar, I. Etxeberria-Otadui, R. Teodoresc, and F. Blaabjerg, "A stationary reference frame grid synchronization system for three-phase grid-connected power converters under adverse grid conditions," *IEEE Trans. Power Electron.*, vol. 27, no. 1, pp. 99–112, Jan. 2012.

[5] S. G. Jorge, C. A. Busada, and J. A. Solsona, "Frequency-adaptive current controller for three-phase grid-connected converters," *IEEE Trans. Ind. Electron.*, vol. 60, no. 10, pp. 4169–4177, Oct. 2013.

[6] R. Chudamani, K. Vasudevan, and C. S. Ramalingam, "Real-time estimation of power system frequency using nonlinear least squares," *IEEE Trans. Power Del.*, vol. 24, no. 3, pp. 1021–1028, Dec. 2009.

[7] M. Qasim, P. Kanjiya, and V. Khadkikar, "Artificial-neural-network-based phase-locking scheme for active power filters," *IEEE Trans. Ind. Electron.*, vol. 61, no. 8, pp. 3857–3866, Aug. 2014.

[8] A. Lopez, J.-C. Montano, M. Castilla, J. Gutierrez, M. D. Borras, and J. C. Bravo, "Power system frequency measurement under non stationary situations," *IEEE Trans. Power Del.*, vol. 23, no. 2, pp. 562–567, Apr. 2008.

[9] P. Roncero-Sanchez, X. del Toro Garcia, A. P. Torres, and V. Feliu, "Robust frequency-estimation method for distorted and imbalanced three-phase systems using discrete filters," *IEEE Trans. Power Electron.*, vol. 26, no. 4, pp. 1089–1101, Apr. 2011.

[10] K. H. Jin and P. N. Markham, "Power system frequency estimation by reduction of noise using three digital filters," *IEEE Trans. Instrum. Meas.*, vol. 63, no. 02, pp. 402–409, Feb. 2014.

[11] R. Yang and H. Xue, "A novel algorithm for accurate frequency measurement using transformed consecutive points of DFT," *IEEE Trans. Power Syst.*, vol. 23, no. 3, pp. 1057–1063, Aug. 2008.

[12] J. Borkowski, D. Kania, and J. Mroczka, "Interpolated-DFT-based fast and accurate frequency estimation for the control of power," *IEEE Trans. Ind. Electron.*, vol. 61, no. 12, pp. 7026–7034, Dec. 2014.

[13] F. Cupertino, E. Lavopa, P. Zanchetta, M. Sumner, and L. Salvatore, "Running DFT-based PLL algorithm for frequency, phase, and amplitude tracking in aircraft electrical systems," *IEEE Trans. Ind. Electron.*, vol. 58, no. 3, pp. 1027–1035, Mar. 2011.

[14] H. Xue, D. Song, and R. Yang, "Consecutive DFT method for instantaneous oscillating phasor measurement," *IEEE Trans. Power Syst.*, vol. 28, no. 4, pp. 4634–4644, Nov. 2013.

[15] Y. Xia, Y. He, K. Wang, W. Pei, Z. Blazic, and D. P. Mandic, "A complex least squares enhanced smart DFT technique for power system frequency estimation," *IEEE Trans. Power Del.*, vol. 32, no. 3, pp. 1270–1278, Jun. 2017.

[16] S. Shinnaka, "A novel fast-tracking D-estimation method for single-phase signals," *IEEE Trans. Power Electron.*, vol. 26, no. 4, pp. 1081–1088, Apr. 2011.

[17] I. Sadinezhad and V. G. Agelidis, "Real-time power system phasors and harmonics estimation using a new decoupled recursive-least-squares technique for DSP implementation," *IEEE Trans. Ind. Electron.*, vol. 60, no. 6, pp. 2295–2308, Jun. 2013.

[18] P. K. Dash and S. Hasan, "A fast recursive algorithm for the estimation of frequency, amplitude, and phase of noisy sinusoid," *IEEE Trans. Ind. Electron.*, vol. 58, no. 10, pp. 4847–4856, Oct. 2, 2011.

[19] M. Karimi-Ghartemani *et al.*, "A new phase-locked loop system for three-phase applications," *IEEE Trans. Power Electron.*, vol. 28, no. 3, pp. 1208–1218, Mar. 2013.

[20] M. K. Ghartemani, S. A. Khajehoddin, P. K. Jain, and A. Bakhshai, "Problems of startup and phase jumps in PLL systems," *IEEE Trans. Power Electron.*, vol. 27, no. 4, pp. 1830–1838, Apr. 2012.

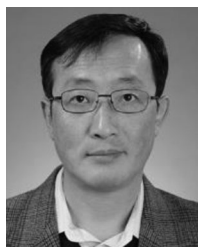

Hongzhi Chen received the B.S. and M.S. degrees in automation in 1986 and 1989, respectively, and the Ph.D. degree in detection technology and automation device in 2012, all from Northeastern University, Shenyang, China. He is currently an Assistant Professor with the Department of Electrical Engineering, Northeastern University. His main research interests include optimal numerical algorithms in the monitoring, operating, and controlling of power systems, as well as control algorithms of grid-connected power electronics devices.

He Chen (S'19) received the B.S. degree in automation from Northeastern University, Shenyang, China, and the M.S. degree in electrical engineering from Tianjin University, Tianjin, China. She is currently working toward the Ph.D. degree with the Whiting School of Engineering, Johns Hopkins University, Baltimore, MD, USA. Her primary research interests include mathematical modeling using group theory, computer vision, and machine learning. At the same time, she is also interested in the control algorithm of systems.